

Semi-classical Description of Exclusive Meson Pair Production in $\gamma^*\gamma$ Scattering

Martin Maul

Institute for Theoretical Physics Lund University, Sölvegatan 14 a, S-223 62 Lund, Sweden

A semi-classical picture is given for the production of exclusive meson pairs in $\gamma^*\gamma$ scattering using elements of the Lund string fragmentation model, spin and C -parity conservation. The model can be generalized to the production of any few meson states in scattering reactions at intermediate momentum transfers. As an example we show that we get a consistent description for the time-like pion form factor. For the reaction $\gamma^*\gamma \rightarrow \pi^+\pi^-$ we find a sizable cross section at LEP2 energies.

PACS: 11.15.Kc, 25.70.Mn, 13.65.+i

Keywords: Lund string model, electron-positron scattering, two-meson fragmentation function.

I. INTRODUCTION

Recently, the factorization of the hadron production process $\gamma^*\gamma \rightarrow h\bar{h}$ in a partonic handbag diagram and a two-hadron distribution amplitude has been discussed [1–3], which describes the exclusive fragmentation of a quark-antiquark pair into two hadrons. This factorization is valid in the kinematic region where the squared c.m. energy of the final hadrons $s = (p + p')^2$ is much smaller than the photon virtuality Q^2 , see Fig. 1. So far, mostly the process $\gamma^*\gamma \rightarrow \pi^+\pi^-$ has been studied and is known to NLO precision [4]. The central object there is the two-pion distribution amplitude [5–7], which has been expressed in terms of the instanton vacuum [8]. The same object enters in terms of hard diffractive electro production of two pions [9,10]. A detailed QCD analyses of the cross section of exclusive production of pion pairs for $s < 1 \text{ GeV}^2$ can be found in [11]. The general process $\gamma^*\gamma \rightarrow \pi^+\pi^-$ has also been studied earlier in the resonance region [12] and in a purely perturbative kinematics involving two light cone wave functions instead of a two-hadron distribution amplitude (2HDA) [13].

In our contribution we want to look at this process from the viewpoint of a semi-classical theory as it was proposed in the Lund model [14]. In a semi-classical theory we will not be able to study the 2HDA. However, the factorization picture motivates a semi-classical description in which a quark-antiquark pair produced by $\gamma^*\gamma$ interaction fluctuates with some probability $P_{q\bar{q} \rightarrow \pi^+\pi^-}(s)$ into a $\pi^+\pi^-$ pair. The two-meson fragmentation function $P_{q\bar{q} \rightarrow \pi^+\pi^-}(s)$ can be evaluated in terms of the string fragmentation picture. Decaying resonances above the mass of $\sqrt{s} = 1 \text{ GeV}$ are treated here as strings. The semi classical picture should be a good approximation when many resonances overlap and interference effects can be neglected.

In the kinematics, where the above mentioned factorization holds, the common picture is that a gluonic string is formed between the quark-antiquark pair and finally breaks into $\pi^+\pi^-$. This process is of special interest because it contains a string breaking exactly one time, and, therefore, it would be a very interesting probe for an understanding of the dynamics of QCD strings. The picture which we are referring to is an incoherent one, because we do not work on the level of amplitudes but of probability densities. This incoherent picture of the Lund string model, as implemented in Monte Carlo (MC) programs like JETSET [15], has been very successful in the description of many particle final states in high-energy physics. It is our aim to investigate what the prediction of this model will be if we reduce the number of final particles to very few ones, actually only two.

In terms of the Lund model few-body states have been discussed only recently [16]. The fragmentation functions used in JETSET [15] only work for high energy processes, where the invariant mass of the string \sqrt{s} is much larger than the masses of the particles produced. In the two-body case the Lund model fixes the fragmentation function only up to a normalizing function $g_{q\bar{q}}(s) = \sum_n g_{q\bar{q} \rightarrow n}(s)$, where $g_{q\bar{q} \rightarrow n}(s)$ describes the (unnormalized) probability that a quark-antiquark string fragments into n particles. In [16] $g_{q\bar{q}}(s)$ was fixed by the requirement that for a given invariant mass squared $s = 4 \text{ GeV}^2$ one should get the same results as the JETSET program, which originally only describes many-body states well. The crucial point is, that especially for two particles the JETSET program is not reliable as it does not contain C -parity for example. In this approach we try to compute $g_{q\bar{q}}(s)$ directly by evaluating the phase space and the string breaking probability for all channels that contribute.

The paper is outlined as follows. In Sec. II we describe the factorization of the cross section $\gamma^*\gamma \rightarrow \pi^+\pi^-$ in terms of Weizsäcker-Williams spectrum, photon structure function and the two-meson fragmentation probability. In Sec. III we will outline how the fragmentation mechanism is understood according to the Lund model plus some minor extensions as to spin and C -parity. Finally, in Sec. IV we will evaluate all competing channels to the $\pi^+\pi^-$ pair production in a region $1 \text{ GeV}^2 < s < 2 \text{ GeV}^2$. We will compare our semi-classical formalism with data from the time-like pion form factor and predict the total cross section $\gamma^*\gamma \rightarrow \pi^+\pi^-$ at LEP2 energies.

II. THE PROCESS $\gamma^*\gamma \rightarrow \pi^+\pi^-$ IN THE SEMI-CLASSICAL THEORY

The kinematics of the process $\gamma^*(q) + \gamma(q_0) \rightarrow h(p) + \bar{h}(p')$ in Fig. 1 has been given in [1] and [2]. The process is governed by the virtuality of the off shell photon $Q^2 = -q^2$ and the invariant mass squared of

the final state hadrons $s = (p + p')^2$. To ensure the factorization according to Fig. 1 we have to satisfy $s \ll Q^2$. Quark-antiquark configurations which have an invariant mass squared $s > 1 \text{ GeV}^2$ are treated in our approach as strings. Below this value the length of the 'string' becomes smaller than 1 fm (with a string constant taken to be $\kappa \approx 1 \text{ GeV/fm}$), and it is not sensible to speak of the configuration as an extended two-dimensional object, as it is then smaller than a typical hadron-radius. A more involved point is the real photon which enters with the momentum q_0 . In principle it can have a substructure in the sense that it fluctuates in to a ρ^0 meson state which interacts then with the virtual γ . This Vector Meson Dominance (VMD) contribution is important for quasi real photons [17].

In this paper we want to look at the process $\gamma^* \gamma \rightarrow \pi^+ \pi^-$ in the sense of Deep Inelastic Scattering (DIS) where the nucleon probe is replaced by a quasi real photon, see e.g. [18]. We treat the exclusive process in the spirit as the MC program LEPTO [19] treats the DIS of electrons off protons: The process $\gamma^* \gamma \rightarrow \pi^+ \pi^-$ factorizes in a handbag diagram including the photon structure function, for which the whole machinery of perturbative QCD is applicable [20–25], and the $\pi^+ \pi^-$ fragmentation function, see Fig. 2.

The production of the initial $q\bar{q}$ pair is given by the handbag diagram of lepton-photon scattering, while the hadronization is given by a probability $P_{q\bar{q} \rightarrow \pi^+ \pi^-}$ that this pair fragments into two pions. The total cross section for the whole process $e^+(l_0) + e^-(l) \rightarrow e^+(l'_0) + e^-(l') + \pi^+(p) + \pi^-(p')$ is then given to leading order accuracy by:

$$\frac{d\sigma(e^+e^- \rightarrow e^+e^-\pi^+\pi^-)}{dy_0 dx dQ_0^2 dQ^2 d^2\mathbf{p}_\perp} = \sum_q e_q^2 \frac{2\pi\alpha_{\text{em}}^2}{Q^4} (1 + (1-y)^2) f_q^\gamma(x, Q^2, Q_0^2) f_{\gamma/e}^T(y_0, Q_0^2) P_{q\bar{q} \rightarrow \pi^+ \pi^-}(s, p_\perp^2).$$

$$y = \frac{q_0 q}{q_0 l}, \quad y_0 = \frac{q_0 l}{l_0 l}, \quad q = l - l', \quad q_0 = l_0 - l'_0, \quad Q^2 = -q^2, \quad Q_0^2 = -q_0^2,$$

$$x = \frac{Q^2}{2q_0 q}, \quad s = (q + q_0)^2 \approx \frac{1-x}{x} Q^2, \quad Q^2 = Sxy_0, \quad S = (l_0 + l)^2. \quad (2.1)$$

$P_{q\bar{q} \rightarrow \pi^+ \pi^-}$ depends on the transverse momentum p_\perp^2 of the two produced pions, which is defined with respect to the axis given by the string spanned by the two initial quarks. However, p_\perp^2 is not a Lorentz invariant quantity. Therefore, from an experimental point of view, one would like to reconstruct the p_\perp^2 -dependence in terms of the Lorentz invariant variables $t = (q - p)^2$ and x , see also Eqs. (4.35) and (4.36). For the definition of the transversity it is furthermore essential, that to leading twist we can define the quark momenta in the framework of the standard parton model in DIS, i.e. that we can express in Fig. 1 $k = xq_0 + q$. The virtuality Q_0^2 of the photon with the 4-momentum q_0 should be small, so that it can be treated as a quasi real photon and the standard approximations in terms of the photo-production formalism are valid.

Also, one should note, that in the convention used here $P_{q\bar{q} \rightarrow \pi^+ \pi^-}(s) = \int P_{q\bar{q} \rightarrow \pi^+ \pi^-}(s, p_\perp^2) d^2\mathbf{p}_\perp$ is a dimensionless quantity. For the factorization to be valid the ordering $Q_0^2 \ll s \ll Q^2$ must be fulfilled. The part of the generation of the (quasi) real photon is described by the standard Weizsäcker-Williams spectrum [26,27] for a transversely polarized photon:

$$f_{\gamma/e}^T(y_0, Q_0^2) = \frac{\alpha_{\text{em}}}{2\pi} \left(\frac{(1 + (1 - y_0)^2)}{y_0} \frac{1}{Q_0^2} - \frac{2m_e^2 y_0}{Q_0^4} \right). \quad (2.2)$$

The contribution of longitudinal polarized photons can be neglected as it is suppressed by one power of Q_0^2 [28].

The $f_q^\gamma(x, Q^2, Q_0^2)$ are the quark parton distributions of the quasi real photon which has the small virtuality Q_0^2 . We will use the parameterization given in [29] [30]. There is one subtlety in using the quark parton distributions of the photon for an approximation of the quasi real photon in our case. Normally, those parton distributions contain also the case that the incoming virtual photon scatters off a quark from the sea. Obviously, in this case the 'photon remnant' is a more complicated object than just an antiquark and it will lead in the end to some more complicated final state than just a $\pi^+ \pi^-$ pair. As we regard

exclusive $\pi^+\pi^-$ pair production, this part of the photon parton distribution is not taken into account in our description. However, we recall here the necessary condition for factorization:

$$x = \frac{Q^2}{Q^2 + s} \approx 1, \quad \text{as } Q^2 \gg s. \quad (2.3)$$

For large x , however, it is known that the parton distributions represent nearly exclusively the valence quarks which correspond in our case just to the valence $q\bar{q}$ pair in the ρ^0 . It means that the photon remnant is then to a very high precision just the corresponding antiquark, carrying the full rest momentum $(1-x)q_0$, and, in this respect, the photon structure function is a good approximation.

$P_{q\bar{q} \rightarrow \pi^+\pi^-}(s)$ is the (semi-classical) probability that the produced $q\bar{q}$ pair fragments into a $\pi^+\pi^-$ state. We will calculate this quantity in terms of the Lund model. For intermediate values of s (as compared to Λ_{QCD}^2) the fragmentation process should be described non-perturbatively. Here the string picture is indisputably valid. For larger and larger s a more perturbative prescription should be valid [13,31], where the second $q\bar{q}$ pair is generated by the branching of a perturbative gluon. In principle, the Lund model should also contain the perturbative contribution, because it describes the generation of the second $q\bar{q}$ pair in a tunneling mechanism which should resume the interaction to all orders. However, the model is an incoherent approximation, so that we cannot expect a one to one correspondence at all. Nevertheless, it will be interesting to study how far the string picture remains valid in this situation.

III. STRING BREAKING AND FRAGMENTATION

In this chapter we want to derive $P_{q\bar{q} \rightarrow \pi^+\pi^-}$ semi-classically. We will pick up some elements from the Lund model as described in [14], but add extensions as to the particle spin and C -parity. The general strategy is to determine $P_{q\bar{q} \rightarrow \pi^+\pi^-}(s)$ by the fraction of the two-meson weight $g_{q\bar{q} \rightarrow \pi^+\pi^-}(s)$ and the total weight $g_{q\bar{q}}(s)$. Here $g_{q\bar{q} \rightarrow \pi^+\pi^-}(s)$ is the weight for the process that the initial $q\bar{q}$ pair fragments into a $\pi^+\pi^-$ pair, and $g_{q\bar{q}}(s)$ is the sum of all n -meson weights for all possible reactions, which the initial $q\bar{q}$ pair can undergo to produce an arbitrary number of mesons. Limiting the value $s < 4 \text{ GeV}^2$ we can neglect any contribution from baryons.

$$P_{q\bar{q} \rightarrow \pi^+\pi^-}(s, p_\perp^2) d^2\mathbf{p}_\perp = \frac{g_{q\bar{q} \rightarrow \pi^+\pi^-}(s, p_\perp^2) d^2\mathbf{p}_\perp}{g_{q\bar{q}}(s)}. \quad (3.4)$$

The term 'weight' denotes a product of the phase space of the given process and its production probability. We will specify these objects in the following. The simplest access is to regard the total weight $g_{q\bar{q}}(s)$. First of all, it is the sum of all weights of the initial $q\bar{q}$ pair producing n mesons:

$$g_{q\bar{q}}(s) = \sum_n g_{q\bar{q} \rightarrow n}(s). \quad (3.5)$$

The n -particle weight is then the sum over all weights where the initial quark-antiquark pair $q\bar{q}$ fragments into n mesons M_1, \dots, M_n :

$$g_{q\bar{q} \rightarrow n}(s) = \sum_{M_1, \dots, M_n} g_{q\bar{q} \rightarrow M_1, \dots, M_n}(s). \quad (3.6)$$

In these weights only meson combinations are included which have the right quantum number with respect to the initial state. For example, in $\gamma^*\gamma$ we have to ensure that the final hadronic state has positive C -parity. In the Lund model approach the production of final state hadrons happens only through string breaking. This means that a resonance like $f_2(1270)$, which is an important intermediate state for the reaction $\gamma^*\gamma \rightarrow \pi^+\pi^-$ [9], is treated in the framework of the string picture. As the string constant κ has the value $\kappa \approx (1 \text{ GeV/fm}) = 0.2 \text{ GeV}^2$ this is a reasonable picture for all mesons with masses above 1 GeV like the $f_2(1270)$ for example, because it means that the distance between the quark-antiquark pair in the meson is considerable larger than 1 fm, which justifies the picture of a string. In fact, the string picture cannot describe resonance poles or interference effects of overlapping resonances as it is an incoherent semi-classical picture. In fact resonances with masses smaller than 1 GeV, namely the ω and ρ resonances,

have to be treated differently as we will show in the case of $e^+e^- \rightarrow \pi^+\pi^-$, see in Sec. IV E. Because of C-parity conservation, ω and ρ resonances are forbidden as intermediate states in exclusive $\gamma^*\gamma$ scattering. However, they make a considerable contribution in the reaction $\gamma^*N \rightarrow \pi^+\pi^- + N$, see [32], and, as we will see later, in the annihilation reaction $e^+e^- \rightarrow \pi^+\pi^-$.

We start now with the description of the two-particle weight $g_{q\bar{q} \rightarrow M_1 M_2}$ with M_1 and M_2 being two mesons.

A. The two-particle weight

The two-meson weight is given by the following formula:

$$\begin{aligned} g_{q\bar{q} \rightarrow M_1 M_2}(s) &= \int d^2 \mathbf{p}_\perp g_{q\bar{q} \rightarrow M_1 M_2}(s, p_\perp^2) \\ &= \int d^2 \mathbf{p}_\perp \int dm_1 P_{\text{mass } M_1}(m_1) \int dm_2 P_{\text{mass } M_2}(m_2) P_{\text{tunnel}}(p_\perp) \\ &\quad \times P_{\text{flavor}}(M_1, M_2) P_{\text{spin}}(M_1) P_{\text{spin}}(M_2) g_2(s, m_{1\perp}^2, m_{2\perp}^2). \end{aligned} \quad (3.7)$$

Here $P_{\text{mass } M_1}(m)$ is the symmetric Breit-Wigner distribution to allow for the fact that some of the mesons considered here, like the ρ , are comparatively broad resonances:

$$P_{\text{mass}}(m) = \frac{1}{2\pi} \frac{\Gamma}{[(m - m_0)^2 + \frac{\Gamma^2}{4}]} . \quad (3.8)$$

$P_{\text{spin}}(M_1)$ gives the probability that the two quarks which are under consideration to form the meson M_1 are coupled to the right spin state. Counting the number of S_z components, the naive values would be:

$$P_{\text{spin}}^{\text{naive}}(S = 0) = \frac{1}{4}, \quad P_{\text{spin}}^{\text{naive}}(S = 1) = \frac{3}{4} . \quad (3.9)$$

However, experimentally, a ratio of pseudoscalar mesons to vector mesons is found that is close to 1:1 [14,33]. One can model this in assuming that for $S = 1$ only one of the three spin degrees of freedom is active leading to the factors

$$P_{\text{spin}}(S = 0) = \frac{1}{4}, \quad P_{\text{spin}}(S = 1) = \frac{1}{4} . \quad (3.10)$$

P_{tunnel} gives the probability for the via string breaking generated quark-antiquark pair to carry the transverse momentum p_\perp with respect to the line of the string. The transverse momentum is generated by tunneling through a linear barrier of length $l = p_\perp/\kappa$, see Fig. 3, with κ being the string constant. The tunneling process can be best understood by considering the situation when the new quark antiquark pair has just been produced. Then the mother string has been split into two new ones. Each of them consists of a quark-antiquark pair sitting in a linear potential. The two linear potentials do not interfere with each other. The distance of the generated quark-antiquark pair is l . The energy of the quantum mechanically forbidden region where this quark-antiquark pair has tunneled through, has been invested in transverse momentum $p_\perp = l\kappa$. To calculate the probability for such a kinematical configuration one has to calculate the overlap of the quark wave functions at the beginning and at the end of the tunneling process. The WKB method predicts for the wave function of one of the quarks in the linear potential:

$$\Psi(x) = \Psi(0) \exp \left[- \int_0^x \sqrt{p_\perp^2 - (\kappa x')^2} dx' \right] . \quad (3.11)$$

One gets the tunneling probability from the normalized square of the overlap of the two density distributions i.e. the square of the two wave functions:

$$P_{\text{tunnel}}(p_\perp) \sim \left| \frac{\Psi(l)}{\Psi(0)} \right|^4 \Leftrightarrow P_{\text{tunnel}}(p_\perp) = \frac{1}{\kappa} \exp \left[- \left(\frac{\pi p_\perp^2}{\kappa} \right) \right] .$$

For the string constant one naively would assume a value $\kappa_{\text{string}} \approx 1 \text{ GeV/fm} \approx 0.2 \text{ GeV}^2$. Again, it turns out in experiment that a somewhat larger value is needed in order to describe the p_{\perp} of hadrons properly [14]. We get a good result in the end for the time-like pion form factor of the pion using a value $\kappa = 0.35 \text{ GeV}^2$ which results in an average hadron transverse momentum of $\langle p_{\perp} \rangle = 0.472 \text{ GeV}$. This is a bit larger than the value $\langle p_{\perp} \rangle = 0.42 \text{ GeV}$ cited in [14]. On the other hand, at the small invariant masses considered here, it is likely that soft effects which could lead to a p_{\perp} smearing are quite important.

$P_{\text{flavor}}(M_1, M_2)$ is the probability to produce the correct flavor for the mesons M_1 and M_2 . From long termed experience with the JETSET program, the following probabilities in the Lund model have been shown to be reasonable [14,15]:

$$P_{\text{flavor}}(d\bar{d}) = P_{\text{flavor}}(u\bar{u}) = 1/2.3, \quad P_{\text{flavor}}(s\bar{s}) = 0.3/2.3. \quad (3.12)$$

The generation of heavy quarks is negligible. For high-energy fragmentation an alternative model has been developed [34] using $P_{\text{flavor}}(d\bar{d}) = P_{\text{flavor}}(u\bar{u}) = P_{\text{flavor}}(s\bar{s}) = 1$. Using this assumption, the final results for the $e^+ + e^- \rightarrow e^+ + e^- + A$ cross sections (with A being a two meson system) Fig. 21 become smaller about 15% for $\rho\rho$ and $\pi\rho$ production. In case of the production of pion pairs the changes are negligible. The same is true for the prediction of the time-like pion form factor Fig. 20. As the overall changes are small we will stick in this contribution to the parameters of the LUND model with the reservation that a precise determination of the strange suppression will be left to a future work on kaon production.

The central objects of the two-particle weights are the two-particle phase space weights $g_2(s, m_{1\perp}^2, m_{2\perp}^2)$. $m_{j\perp}$ denotes the transverse mass, i.e., $m_{j\perp}^2 = m_j^2 + p_{j\perp}^2$. For a concise treatment one has to regard the general n -particle phase space weights $g_n(s, m_{1\perp}^2, \dots, m_{n\perp}^2)$ first.

B. n -particle weights

The n -particle weights $g_{q\bar{q} \rightarrow n}(s)$ can be derived by means of the n -particle phase space weights $g_n(s, m_{1\perp}^2, \dots, m_{n\perp}^2)$ which are given according to the Lund model [14]:

$$g_n(s, m_{1\perp}^2, \dots, m_{n\perp}^2) = \prod_{j=1}^n N_j d^2\mathbf{p}_j \delta(p_j^2 - m_{j\perp}^2) \delta\left(\sum_j p_j - (\sqrt{s}, 0)\right) \exp(-bA). \quad (3.13)$$

A is the shaded area spanned by the particle momenta shown in Fig. 4. b is one of the two parameters in the Lund model which have to be fitted to experimental data. The value used for the calculations is $b = 0.75 \text{ GeV}^{-2}$ [35]. $m_{j\perp}^2 = m_j^2 + p_{j\perp}^2$ is the transverse mass of the j -th particle. One should observe that the phase space weight is independent of the flavor q . We will see later how n -particle weights and n -particle phase space weights fit together. N_j can be interpreted as a sort of coupling constant for the j th particle. It can be fixed by a simple iterative condition. The two-particle phase space weight gives a simple analytic expression [16]: It is constructed from energy momentum conservation (see Fig. 5):

$$m_{2\perp}^2 = (1 - z) \left(s - \frac{m_{1\perp}^2}{z} \right), \quad (3.14)$$

which yields:

$$z_{\pm} = \frac{s + m_{1\perp}^2 - m_{2\perp}^2 \pm \sqrt{\lambda(s, m_{1\perp}^2, m_{2\perp}^2)}}{2s}$$

$$\lambda(x, y, z) = x^2 + y^2 + z^2 - 2xy - 2xz - 2yz. \quad (3.15)$$

The area is then given by (see Fig. 5):

$$\mathcal{A}_{\pm} = m_{2\perp}^2 + \frac{m_{1\perp}^2}{z_{\pm}} = m_{2\perp}^2 + s z_{\mp} = \frac{1}{2} \left(s + m_{1\perp}^2 + m_{2\perp}^2 \mp \sqrt{\lambda(s, m_{1\perp}^2, m_{2\perp}^2)} \right). \quad (3.16)$$

Furthermore, one has also:

$$\int d^2\mathbf{p}_1 \int d^2\mathbf{p}_2 \delta(p_1^2 - m_{1\perp}^2) \delta(p_2^2 - m_{2\perp}^2) \delta(p_1 + p_2 - (\sqrt{s}, 0)) = \frac{1}{\sqrt{\lambda(s, m_{1\perp}^2, m_{2\perp}^2)}}, \quad (3.17)$$

which yields the analytic result for the two-particle phase space weight:

$$g_2(s, m_{1\perp}^2, m_{2\perp}^2) = N_1, N_2 \frac{2 \exp\left[-\frac{b}{2}(s + m_{1\perp}^2 + m_{2\perp}^2)\right]}{b \sqrt{\lambda(s, m_{1\perp}^2, m_{2\perp}^2)}} \cosh\left(\frac{b}{2} \sqrt{\lambda(s, m_{1\perp}^2, m_{2\perp}^2)}\right). \quad (3.18)$$

We included a factor b in the denominator to get an dimensionless expression. The cosh corresponds to two possible solutions that obey energy momentum conservation when the two-dimensional string breaks into two parts. Then the other phase space weights can be obtained iteratively via [36]:

$$g_n(s, m_{1\perp}^2, \dots, m_{n\perp}^2) = N_n \int \frac{dz}{z} \exp\left(\frac{-bm_{n\perp}^2}{z}\right) g_{n-1}\left[(1-z)\left(s - \frac{m_{n\perp}^2}{z}\right), m_{1\perp}^2, \dots, m_{n-1\perp}^2\right]. \quad (3.19)$$

This equation is also suitable to fix N_j . In the Lund model the N_j are universal constants only dependent on $m_{j\perp}$, but not on s to ensure left right symmetry. The idea is [36] that after summation over n on both sides, the iterative equation has a solution in form of $\sum_n g_n(s, *) \sim s^a$ for asymptotically large s , which yields then in this limit:

$$\begin{aligned} N_j &= N(a, bm_{j\perp}^2) = \lim_{s \rightarrow \infty} \left\{ 1 / \int_{m_{1j}^2/s}^1 \frac{dz}{z} (1-z)^a \exp\left(\frac{-bm_{j\perp}^2}{z}\right) \left(1 - \frac{m_{j\perp}^2}{sz}\right)^a \right\} \\ &= 1 / \int_0^1 \frac{dz}{z} (1-z)^a \exp\left(\frac{-bm_{j\perp}^2}{z}\right). \end{aligned} \quad (3.20)$$

a is the second parameter in the Lund model. The value, which we will use in our calculation, is $a = 0.5$ [35].

C. The weights for n mesons

The procedure described in the previous two subsections can easily be generalized to describe the weight to produce n mesons M_1, \dots, M_n from one mother string:

$$\begin{aligned} g_{q\bar{q} \rightarrow M_1, \dots, M_n}(s) &= \left[\prod_{j=1}^{n-1} \int d^2\mathbf{p}_{j\perp} P_{\text{tunnel}}(p_{j\perp}) \right] \left[\prod_{i=1}^n \int dm_i P_{\text{mass}, M_i}(m_i) P_{\text{spin}}(M_i) \right] \\ &\times g_n(s, m_{1\perp}^2, \dots, m_{n\perp}^2) P_{\text{flavor}}(M_1, \dots, M_n). \end{aligned} \quad (3.21)$$

One should then observe that:

$$\begin{aligned} m_{1\perp}^2 &= m_1^2 + p_{1\perp}^2; \\ m_{i\perp}^2 &= m_i^2 + (p_{i-1\perp} - p_{i\perp})^2, \quad (1 < i < n); \\ m_{n\perp}^2 &= m_n^2 + p_{n-1\perp}^2. \end{aligned} \quad (3.22)$$

In practice, it will be easier to make use of the recurrence relation. Here the three-meson phase space weight is given by:

$$g_3(s, m_{1\perp}^2, m_{2\perp}^2, m_{3\perp}^2) = N(a, bm_{3\perp}^2) \int \frac{dz}{z} \exp\left(-\frac{bm_{3\perp}^2}{z}\right) g_2\left((1-z)\left[s - \frac{m_{3\perp}^2}{z}\right], m_{1\perp}^2, m_{2\perp}^2\right). \quad (3.23)$$

What causes problems numerically, is the integration over the transverse momenta. The kinematic situation is the one of Fig. 6, i.e., that the particle in the middle receives transverse momentum from two string break points, whereas a particle at the end only from one. To simplify things we will take average values instead of a time consuming p_{\perp} integration. First, the average over the relative orientation of the transverse vectors yields:

$$(p_{1\perp} - p_{2\perp})^2 \approx p_{1\perp}^2 + p_{2\perp}^2 . \quad (3.24)$$

To simplify things further, we will also replace $p_{1\perp}^2 \approx \langle p_{1\perp}^2 \rangle = \kappa/\pi$ for one of the three particles. Taking into account that each of the three particles may sit in mid position in Fig. 6, we get:

$$\begin{aligned} & g_{q\bar{q} \rightarrow M_1 M_2 M_3}(s, m_1^2, m_2^2, m_3^2) \\ &= \int \frac{dz}{z} \left[e^{-\frac{b(m_3^2 + 2\kappa/\pi)}{z}} N(a, b(m_3^2 + 2\kappa/\pi)) g_{q\bar{q} \rightarrow M_1 M_2} \left((1-z) \left(s - \frac{m_3^2 + 2\kappa/\pi}{z} \right), m_1^2, m_2^2 \right) \right. \\ & \quad + e^{-\frac{b(m_3^2 + \kappa/\pi)}{z}} N(a, b(m_3^2 + \kappa/\pi)) g_{q\bar{q} \rightarrow M_1 M_2} \left((1-z) \left(s - \frac{m_3^2 + \kappa/\pi}{z} \right), m_1^2 + \kappa/\pi, m_2^2 \right) \\ & \quad \left. + e^{-\frac{b(m_3^2 + \kappa/\pi)}{z}} N(a, b(m_3^2 + \kappa/\pi)) g_{q\bar{q} \rightarrow M_1 M_2} \left((1-z) \left(s - \frac{m_3^2 + \kappa/\pi}{z} \right), m_1^2, m_2^2 + \kappa/\pi \right) \right] \\ & \times P_{\text{spin}}(M_3) P_{\text{flavor}} . \end{aligned} \quad (3.25)$$

Here, we have taken advantage of the fact that the functions $g_n(s, m_{1\perp}^2, \dots, m_{n\perp}^2)$ are symmetric under permutation of the $m_{i,\perp}^2$ up to a finite energy correction. We will check later to which extent this symmetry is fulfilled. Furthermore, we have to state that this approximation is only valid because we will restrict ourselves to u and d -quarks. Strange quarks would lead to at least two kaons plus a third meson and this will not contribute in the range $1 \text{ GeV}^2 < s < 2 \text{ GeV}^2$. One has to take into account that one has to deal with transverse masses here, i.e. one has to add the average transverse momentum, which is roughly $1/3 \text{ GeV}$ per contributing quark in our case. If one calculates the weight for $KK\pi$ production, for example, one will observe that its shape resembles essentially the one of the $\pi\pi\eta'$ contribution in Fig. 14, which starts around $s = 2 \text{ GeV}^2$. Neglecting the $KK\pi$ and corresponding channels, the expression Eq. (3.25) is basically flavor independent, as u and d quarks are treated equal because of their small mass difference. Otherwise we would be in trouble because the initial quark-antiquark pair in the two-meson weight and the three-meson weight are not identical. Our three-meson weight contains then all three possible combinations of the three particles being formed along the line of a string breaking two times. One finds analogously for the four-meson weight:

$$\begin{aligned} & g_{q\bar{q} \rightarrow M_1 M_2 M_3 M_4}(s, m_1^2, m_2^2, m_3^2, m_4^2) \\ &= \int \frac{dz}{z} \left[2e^{-\frac{b(m_4^2 + 2\kappa/\pi)}{z}} N(a, b(m_4^2 + 2\kappa/\pi)) g_{q\bar{q} \rightarrow M_1 M_2 M_3} \left((1-z) \left(s - \frac{m_4^2 + 2\kappa/\pi}{z} \right), m_1^2, m_2^2, m_3^2 \right) \right. \\ & \quad + \frac{2}{3} e^{-\frac{b(m_4^2 + \kappa/\pi)}{z}} N(a, b(m_4^2 + \kappa/\pi)) g_{q\bar{q} \rightarrow M_1 M_2 M_3} \left((1-z) \left(s - \frac{m_4^2 + \kappa/\pi}{z} \right), m_1^2 + \kappa/\pi, m_2^2, m_3^2 \right) \\ & \quad + \frac{2}{3} e^{-\frac{b(m_4^2 + \kappa/\pi)}{z}} N(a, b(m_4^2 + \kappa/\pi)) g_{q\bar{q} \rightarrow M_1 M_2 M_3} \left((1-z) \left(s - \frac{m_4^2 + \kappa/\pi}{z} \right), m_1^2, m_2^2 + \kappa/\pi, m_3^2 \right) \\ & \quad \left. + \frac{2}{3} e^{-\frac{b(m_4^2 + \kappa/\pi)}{z}} N(a, b(m_4^2 + \kappa/\pi)) g_{q\bar{q} \rightarrow M_1 M_2 M_3} \left((1-z) \left(s - \frac{m_4^2 + \kappa/\pi}{z} \right), m_1^2, m_2^2, m_3^2 + \kappa/\pi \right) \right] \\ & \times P_{\text{spin}}(M_4) P_{\text{flavor}} . \end{aligned} \quad (3.26)$$

The factors take into account that the fourth particle has two possibilities to sit at the head of the string and two possibilities to sit the midst, see Fig. 6.

IV. NUMERICAL ESTIMATES

A. Two-meson weights

Fig. 7 shows the weight $g_{u\bar{u}\rightarrow\pi^+\pi^-}(s = 1 \text{ GeV}^2, p_{\perp}^2)$. The region in p_{\perp}^2 is limited by the requirement that $\lambda^2(s, m_{1\perp}^2, m_{2\perp}^2) > 0$. One encounters from the phase-space an integrable singularity at:

$$p_{\perp}^2 = \frac{1}{4} \left[s - 2(m_1^2 + m_2^2) + \frac{(m_1^2 - m_2^2)^2}{s} \right]. \quad (4.27)$$

We have to calculate all possible two-meson weights. As we will restrict to a comparatively small region in s , i.e. $1 \text{ GeV}^2 < s < 2 \text{ GeV}^2$, we will only take into account the lightest pseudoscalar mesons and vector mesons. As we are only interested in $\pi^+\pi^-$ production we have to regard for the principal quark-antiquark pair only the flavors u and d . As heavy quarks are actually not generated in fragmentation we can exclude all mesons carrying charm, bottom and of course top quarks. In our formalism, an $s\bar{s}$ pair can only be generated through string breaking, and consequently, it cannot recombine to a Φ meson, as the two strange quarks belong to different strings. Therefore, the generation of an $s\bar{s}$ pair in fragmentation leads exclusively to kaon pairs, while the $d\bar{d}$ and $u\bar{u}$ pairs only produce pions, rhos, etas, and omegas. Φ mesons are neglected altogether because they consist to almost 100% of $s\bar{s}$ [37]. According to recent analysis [38–40], the η meson consists to 40% of $s\bar{s}$ and the η' meson to 60% of $s\bar{s}$. This means that we have to weight the η production by a factor 3/5 and the η' production by a factor 2/5.

For neutral particles that are their own antiparticles we have to take into account that the final state must be in total $C = +$. This leads to the possible combinations in Tab. I. The masses and widths used for the computation are given in Tab. II. In fact, the Breit-Wigner distribution has to be taken into account only for the vector mesons.

Fig. 8 shows the contributions from the charged non strange sector, i.e. the combinations π^{\pm}, ρ^{\pm} . In general, vector mesons have a larger mass than their pseudoscalar partners. Therefore, their weight starts later in s , where there is more competition with other channels. One sees later that this suppresses the contribution of the ρ .

Fig. 9 shows the two-meson weights for the neutral $C = +$ mesons. One observes that due to the strange content of the η and η' mesons their weight is suppressed. The neutral $C = -$ sector consists only of combinations of ρ^0 and ω mesons. Their masses are close to each other, so the only effect visible comes from their different widths, see Fig. 10. In case of the mixed combinations (one vector meson and one pseudoscalar meson) we observe both effects: the suppression of the contribution from the η and η' mesons on the one hand and the fact, that ρ^0 and ω mesons basically can be only distinguished according to their widths, on the other hand (Fig. 11). The mixed combinations will not contribute in $\gamma^*\gamma$ scattering because of C -parity conservation, but they will contribute to other processes like e^+e^- annihilation. For the strange meson contribution (Fig. 12) one observes the suppression of the strangeness production versus the production of $u\bar{u}$ and $d\bar{d}$ pairs.

It is very interesting to investigate the dependence of our results on the parameters a and b in the Lund model. In Fig. 13 we show again the function $g_{u\bar{u}\rightarrow\pi^+\pi^-}(s)$ with a varying between $0.4 < a < 0.6$ and b varying between $0.65 \text{ GeV}^{-2} < b < 0.85 \text{ GeV}^{-2}$. The parameter a accounts for most of the uncertainty. In general, the deviations are small. This means that the results are relatively insensitive to the choice of a and b .

From the results obtained so far, we can compute the total two-meson or two-particle weight function. In case of a $C = +$ state it is given by:

$$g_{u\bar{u}\rightarrow 2}^{(+)}(s) = g_{u\bar{u}\rightarrow\pi^+\pi^-}(s) + g_{u\bar{u}\rightarrow\pi^+\rho^-}(s) + g_{u\bar{u}\rightarrow\rho^+\pi^-}(s) + g_{u\bar{u}\rightarrow\rho^+\rho^-}(s)$$

$$\begin{aligned}
& +g_{u\bar{u}\rightarrow\pi^0\pi^0}(s) + g_{u\bar{u}\rightarrow\eta\eta}(s) + g_{u\bar{u}\rightarrow\eta'\eta'}(s) \\
& +2g_{u\bar{u}\rightarrow\pi^0\eta}(s) + 2g_{u\bar{u}\rightarrow\pi^0\eta'}(s) + 2g_{u\bar{u}\rightarrow\eta\eta'}(s) \\
& +g_{u\bar{u}\rightarrow\rho^0\rho^0}(s) + g_{u\bar{u}\rightarrow\omega\omega}(s) + 2g_{u\bar{u}\rightarrow\rho^0\omega}(s) \\
& +g_{u\bar{u}\rightarrow K^+K^-}(s) + g_{u\bar{u}\rightarrow K^+K^{*-}}(s) + g_{u\bar{u}\rightarrow K^{*+}K^-}(s) + g_{u\bar{u}\rightarrow K^{*+}K^{*-}}(s) ; \tag{4.28}
\end{aligned}$$

and in case of a $C = -$ state by:

$$\begin{aligned}
g_{u\bar{u}\rightarrow 2}^{(-)}(s) & = g_{u\bar{u}\rightarrow\pi^+\pi^-}(s) + g_{u\bar{u}\rightarrow\pi^+\rho^-}(s) + g_{u\bar{u}\rightarrow\rho^+\pi^-}(s) + g_{u\bar{u}\rightarrow\rho^+\rho^-}(s) \\
& +2g_{u\bar{u}\rightarrow\pi^0\rho^0}(s) + 2g_{u\bar{u}\rightarrow\eta\rho^0}(s) + 2g_{u\bar{u}\rightarrow\eta'\rho^0}(s) \\
& +2g_{u\bar{u}\rightarrow\pi^0\omega}(s) + 2g_{u\bar{u}\rightarrow\eta\omega}(s) + 2g_{u\bar{u}\rightarrow\eta'\omega}(s) \\
& +g_{u\bar{u}\rightarrow K^+K^-}(s) + g_{u\bar{u}\rightarrow K^+K^{*-}}(s) + g_{u\bar{u}\rightarrow K^{*+}K^-}(s) + g_{u\bar{u}\rightarrow K^{*+}K^{*-}}(s) . \tag{4.29}
\end{aligned}$$

In the case $g_{d\bar{d}\rightarrow 2}^{(\pm)}(s)$ only the contribution of the charged kaons has to be replaced by neutral kaons.

B. Three-meson weights

For the three-meson weights we make use of the approximation Eq. (3.25). We will only take into consideration the lightest mesons. In case of neutral particles we get again limitations because of C -parity conservation, thus reducing the number of possible combinations to the following for a $C = +$ state:

$$\begin{aligned}
& \pi^+\pi^-\pi^0, \pi^0\pi^0\pi^0, \\
& \pi^+\pi^-\eta, \pi^0\pi^0\eta, \\
& \pi^+\pi^-\eta', \pi^0\pi^0\eta', \\
& \pi^+\pi^-\rho^0, \pi^+\pi^-\omega, \\
& \pi^+\pi^0\rho^-, \pi^-\pi^0\rho^+;
\end{aligned}$$

and to

$$\begin{aligned}
& \pi^+\pi^-\rho^0, \pi^0\pi^0\rho^0, \\
& \pi^+\pi^-\omega, \pi^0\pi^0\omega, \\
& \pi^+\pi^-\pi^0, \\
& \pi^+\pi^-\eta, \pi^+\pi^-\eta', \\
& \pi^+\pi^0\rho^-, \pi^-\pi^0\rho^+
\end{aligned}$$

for a $C = -$ state. We put the heaviest particle always at position 3 in Eq. (3.25) because this is the position where the approximation $p_\perp^2 \approx \langle p_\perp^2 \rangle = \kappa/\pi$ takes place and the error should be proportional to p_\perp^2/m^2 . Fig. 14 shows the various three-meson contributions. A quite substantial contribution comes from the combinations $\pi\pi\rho$ and $\pi\pi\omega$.

It is important to make a check of the reliability of the approximation. In Eq. (3.25) the meson in the position 3 is treated different from the mesons at position 2 and 1. We will have a brief look what consequences this asymmetry has. In Fig. 15 we show for the combination $\pi^0\pi^0\eta$ the two possibilities: One time the η holds position three as in the calculation and one time it is on position 2 or 1, respectively. One observes that the absolute magnitude does not change much, but that when η sits on position 2 or 1 the weight starts later in s . From the calculated three-meson weights we can compute the three-particle weight, which is in case of a $C = +$ state:

$$\begin{aligned}
g_{u\bar{u}\rightarrow 3}^{(+)}(s) & = g_{u\bar{u}\rightarrow\pi^+\pi^-\pi^0}(s) + g_{u\bar{u}\rightarrow\pi^0\pi^0\pi^0}(s) \\
& +g_{u\bar{u}\rightarrow\pi^+\pi^-\eta}(s) + g_{u\bar{u}\rightarrow\pi^0\pi^0\eta}(s)
\end{aligned}$$

$$\begin{aligned}
& +g_{u\bar{u}\rightarrow\pi^+\pi^-\eta'}(s) + g_{u\bar{u}\rightarrow\pi^0\pi^0\eta'}(s) \\
& +g_{u\bar{u}\rightarrow\pi^-\pi^0\rho^+}(s) + g_{u\bar{u}\rightarrow\pi^+\pi^0\rho^-}(s) + g_{u\bar{u}\rightarrow\pi^+\pi^-\rho^0}(s) + g_{u\bar{u}\rightarrow\pi^+\pi^-\omega}(s) .
\end{aligned} \tag{4.30}$$

The corresponding expression for the $C = -$ state is trivial.

C. Four-meson weights

For the four-meson contribution we take into account only pions because they are the lightest particles. Then the following combinations contribute:

$$\pi^+\pi^-\pi^+\pi^-, \quad \pi^+\pi^-\pi^0\pi^0, \quad \pi^0\pi^0\pi^0\pi^0 . \tag{4.31}$$

Because of the small mass difference the weights of the three combinations are practically indistinguishable, so it is sufficient to calculate one of them. Again, we make use of the recurrence relation Eq. (3.26). Fig. 16 shows the weight for the case $\pi^0\pi^0\pi^0\pi^0$, but it is indistinguishable from any other possible combination with charged pions. It is seen that the four-meson weight numerically only becomes relevant for $s > 2 \text{ GeV}^2$. Therefore, no four-meson weights or even higher weights are taken into account in our calculation.

D. The total weight function and the $q\bar{q} \rightarrow \pi^+\pi^-$ fragmentation function

Now we can compute the total weight function relevant in the region $s < 2 \text{ GeV}^2$ or with some reservations also to $s < 2.5 \text{ GeV}^2$. Fig. 17 shows the total weight $g_{u\bar{u}}(s) \approx g_{u\bar{u}\rightarrow 2}^{(+)}(s) + g_{u\bar{u}\rightarrow 3}^{(+)}(s)$ for the $\gamma^*\gamma$ reaction. The weight $g_{d\bar{d}}(s)$ cannot be distinguished from $g_{u\bar{u}}(s)$ as the mass difference between charged and neutral kaons is negligible. One observes that in the region $1 \text{ GeV}^2 < s < 2.5 \text{ GeV}^2$ the correction of the three-meson weights is substantial. The same observations hold also for the total $C = -$ weight, which is not displayed here.

Fig. 18 shows the $\gamma^*\gamma$ fragmentation probabilities $P_{q\bar{q}\rightarrow\pi\pi}(s)$, $P_{q\bar{q}\rightarrow\pi\rho}(s)$, and $P_{q\bar{q}\rightarrow\rho\rho}(s)$, where q can be an u or a d quark. One observes an effective suppression for the production of ρ mesons. The reason lies in the fact that the ρ resonance appears later in s , where there is more competition with other channels. One should bear in mind that the primary production ratio between pseudoscalar and vector mesons in the model is 1:1.

E. Comparison to the time-like pion form factor

It is interesting to confront our mechanism with data one knows from the time-like pion form factor $F_\pi(s)$. In the region $1 \text{ GeV}^2 < s < 4 \text{ GeV}^2$ one has data from Novosibirsk [41] and the DM2 Collaboration [42]. Here the pion form factor is measured in the e^+e^- annihilation process where the cross section is given let alone from mass corrections by (see [43,44]):

$$\sigma(e^+e^- \rightarrow \pi^+\pi^-)(s) = \frac{\pi\alpha_{\text{em}}^2}{3s} |F_\pi(s)|^2 . \tag{4.32}$$

In our approach, this should be the same as the cross section for the annihilation reaction $e^+e^- \rightarrow q\bar{q}$ times the subsequent fragmentation probability into the $\pi^+\pi^-$ pair (see Fig. 19):

$$\sigma(e^+e^- \rightarrow \pi^+\pi^-)(s) = \sum_q \sigma(e^+e^- \rightarrow q\bar{q})(s) P_{q\bar{q}\rightarrow\pi^+\pi^-}^{(-)}(s) = \sum_q \frac{4\pi\alpha_{\text{em}}^2}{s} e_q^2 \frac{g_{q\bar{q}\rightarrow\pi^+\pi^-}(s)}{g_{q\bar{q}}^{(-)}(s)} . \tag{4.33}$$

In contrast to the production of two pions from $\gamma^*\gamma$, the final state in e^+e^- annihilation must have the quantum number $C = -$. This means that we have to take a total weight function $g_{q\bar{q}}^{(-)}(s)$ which includes all relevant $C = -$ states. Our model will be a good description for the decay of resonances with masses larger than 1 GeV , where the resonance can be interpreted as a string. In order to compare with data we

have to include the fact that because of the final state being of $C = -$ a considerable contribution comes from the decay of one $\rho(770)$ meson (neglecting the G parity violating transitions $\omega, \Phi \rightarrow \pi\pi$). We can take into consideration this contribution via the Vector Meson Dominance model (VMD) [45]:

$$|F_\pi(s)|_{\text{VMD}}^2 = \frac{g_{\rho\gamma}^2 g_{\rho\pi\pi}^2}{(s - m_\rho^2)^2 + \frac{m_\rho^6 \Gamma_\rho^2}{s^2} \left(\frac{s - 4m_\pi^2}{m_\rho^2 - 4m_\pi^2} \right)^3}. \quad (4.34)$$

We take the value $g_{\rho\gamma} g_{\rho\pi\pi} = 0.705$ [46,47]. In Fig. 20 it is shown that adding the string fragmentation contribution to the VMD contribution yields a qualitatively good semi-classical description of the time like pion form factor. Of course the incoherent ansatz cannot model the interference structure of the resonances, but it gives a good description on the average, exactly what this semi-classical picture should be.

F. The process $\gamma^* \gamma \rightarrow \pi^+ \pi^-$ at LEP2

Finally, we calculate the $\gamma^* \gamma \rightarrow \pi^+ \pi^-$ cross section. As a small digression we want to show how to reconstruct p_\perp from Lorentz-invariant and experimentally accessible quantities. Defining the variables $t = (p - q)^2$, $t' = (p - k)^2$, and $k = xq_0 + q$ we get the relation:

$$\begin{aligned} t' &= m_\pi^2 - 2pk \\ &= m_\pi^2 - 2 \left(\frac{1}{2} \sqrt{s}, \vec{p}_\perp, \sqrt{\frac{1}{4} - \frac{m_{\pi\perp}^2}{s}} \sqrt{s} \right) \left(\frac{1}{2} \sqrt{s}, \vec{0}, \frac{1}{2} \sqrt{s} \right) \\ &= -(sz - m_\pi^2) = (1 - x)t + xm_\pi^2. \end{aligned} \quad (4.35)$$

Then for the total cross section one can in principle rewrite the p_\perp dependence as follows:

$$\begin{aligned} \frac{d\sigma(ee \rightarrow ee\pi^+\pi^-)}{dy_0 ds dQ_0^2 dQ^2 d^2\mathbf{p}_\perp} &= \sum_q e_q^2 \frac{2\pi\alpha_{\text{em}}^2}{Q^6} \frac{(1 + (1 - y)^2)}{(1 + s/Q^2)^2} f_q^\gamma(x, Q^2, Q_0^2) f_{\gamma/e}^T(y_0, Q_0^2) P_{q\bar{q} \rightarrow \pi^+\pi^-}(s, p_\perp^2) \\ \frac{d\sigma(ee \rightarrow ee\pi^+\pi^-)}{dy_0 ds dQ_0^2 dQ^2 dt} &= \sum_q e_q^2 \frac{2\pi\alpha_{\text{em}}^2}{Q^6} (1 + (1 - y)^2) f_q^\gamma(x, Q^2, Q_0^2) f_{\gamma/e}^T(y_0, Q_0^2) \\ &\quad \times \pi \frac{s/Q^2}{(1 + s/Q^2)^3} \sqrt{1 - 4 \frac{m_{\pi\perp}^2}{s}} P_{q\bar{q} \rightarrow \pi^+\pi^-}(s, p_\perp^2), \quad p_\perp^2 = sz(1 - z) - m_\pi^2. \end{aligned} \quad (4.36)$$

So, p_\perp^2 can be reconstructed from t, s , and Q^2 . Unfortunately, the luminosity that we will consider here is not sufficient to trace the p_\perp dependence of the cross section. But we can instead have a look at the s dependence of the total p_\perp -integrated cross section. For the numerical integration we use the standard LEP-2 parameters [23] with a luminosity $\mathcal{L} = 500 \text{ pb}^{-1}$ and the e^+e^- center of mass energy $\sqrt{S} = 175 \text{ GeV}$. For Q^2 the allowed and measurable range is $5 \text{ GeV}^2 < Q^2 < 500 \text{ GeV}^2$. For the lower boundary of Q^2 we have to choose a rather low value in order to get a considerable rate, although higher-twist contributions may be quite important here. For the other cuts we choose:

$$\begin{aligned} 0.01 < y_0 < 0.99 \\ 1 \text{ GeV}^2 < s < 2.5 \text{ GeV}^2. \end{aligned} \quad (4.37)$$

We approximate the total cross section with the Q_0^2 integrated Weizsäcker-Williams spectrum [48]:

$$f_{\gamma/e}^T(y, Q_{\text{WW}}^2) = \frac{\alpha_{\text{em}}}{2\pi} \left[\frac{(1 + (1 - y)^2)}{y} \ln \frac{Q_{\text{WW}}^2(1 - y)}{m_e^2 y^2} + 2m_e^2 y \left(\frac{1}{Q_{\text{WW}}^2} - \frac{1 - y}{m_e^2 y^2} \right) \right]. \quad (4.38)$$

We choose for the Weizsäcker-Williams scale $Q_{\text{WW}}^2 = (m_1 + m_2)^2$, where m_1 and m_2 are the masses of the two mesons produced [48,49], hereby assuming that the maximum virtuality of the quasi real photon is smaller than 0.09 GeV^2 . For the electromagnetic coupling constant we choose a constant value $\alpha_{\text{em}} = 1/137$. Then, we get the approximated (and p_{\perp} -integrated) formula:

$$\frac{d\sigma(ee \rightarrow ee\pi^+\pi^-)}{dy_0 ds dQ^2} \approx \sum_q e_q^2 \frac{2\pi\alpha_{\text{em}}^2}{Q^6} \frac{(1 + (1-y)^2)}{(1 + s/Q^2)^2} f_q^\gamma(x, Q^2, 0 \text{ GeV}^2) f_{\gamma/e}^T(y_0, Q_{\text{WW}}^2) P_{q\bar{q} \rightarrow \pi^+\pi^-}(s), \quad (4.39)$$

using again

$$P_{q\bar{q} \rightarrow \pi^+\pi^-}(s) = \int d^2\mathbf{p}_{\perp} P_{q\bar{q} \rightarrow \pi^+\pi^-}(s, p_{\perp}^2). \quad (4.40)$$

For the photon structure function we choose the set SAS2 ($\overline{\text{MS}}$ scheme) [29,30]. Fig. 21 shows the cross section for the LEP2 parameters above. In the given kinematical range the contribution of $\pi^+\rho^-$ dominates over the $\pi^+\pi^-$ one.

Experimentally, exclusive $\gamma^*\gamma$ scattering is a subprocess of the more general exclusive $e\gamma$ scattering, see Fig. 22: Taking the process $e\gamma \rightarrow e\pi^+\pi^-$ for example, the measurable cross section consists of a contribution from $\gamma^*\gamma$ scattering (Fig. 22(a)), and a background process of bremsstrahlung (Fig. 22(b)). The cross sections for both reactions have been estimated in [11]. We can use their model predictions and calculations for the cross section $d\sigma_{e\gamma \rightarrow e\pi^+\pi^-}/(dsdQ^2)$ to compare with our results of the Lund model, see Fig. 23. Here we have plotted the Lund model prediction for $\gamma^*\gamma$ scattering versus the result for $\gamma^*\gamma$ scattering and the bremsstrahlung background from [11] for three different values of Q^2 , choosing for the invariant mass of the photon-electron system $\sqrt{S_{e\gamma}} = 60 \text{ GeV}$. It turns out that at the matching point $s = 1 \text{ GeV}^2$ the Lund model prediction is a factor 3.5 larger than the model prediction in [11]. The discrepancy increases to a factor of nearly 5 if one goes down to $s = 0.8 \text{ GeV}^2$, but at that value of s it is doubtful whether the Lund model is reliable any longer. Considering that the model assumptions made in our case are still crude and that in [11] they estimate their model to be correct roughly by a factor of 2, the discrepancy is tolerable, and the model predictions shown here will be improved as soon as data are available. One can conclude, that the bremsstrahlung contribution is also negligible for $Q^2 < 100 \text{ GeV}^2$ and $s > 1 \text{ GeV}^2$. The interference contribution between $\gamma^*\gamma$ scattering and bremsstrahlung vanishes if one integrates over the azimuthal angle between the planes defined by the in and outgoing lepton on the one hand and the two produced pions on the other hand, which we have done here.

V. SUMMARY AND CONCLUSIONS

In this contribution we described the production of two-meson states at intermediate momentum transfers in a semi-classical picture using elements of the Lund model. In contrast to the well known application of this model to high energy physics we counted all states explicitly and took spin and C -parity into consideration. The model gives a fairly good description at intermediate momentum transfers above 1 GeV^2 when the decay of meson resonances can be identified with the breaking of a string. This can be seen from the fact that we get a consistent description for the time-like pion form factor averaging over all interference effects. The procedure has the potential to be the basis of a Monte Carlo program for intermediate energies. As an application we have used this picture to predict the cross section $\gamma^*\gamma \rightarrow \pi^+\pi^-$, which is interesting because it is sensitive to the two-particle distribution amplitude and offers the possibility to observe the decay of a single string and the formation of hadrons from quarks. The cross section should be sizable at LEP2.

Acknowledgment: The author acknowledges stimulating discussion with B. Andersson, J. Bijnens, G. Gustafson, L. Lönnblad and T. Sjöstrand, and especially with M. Diehl, who also sent the program for the comparison of his model with the calculations performed in the Lund model.

-
- [1] M. Diehl, T. Gousset, B. Pire and O. Teryaev, Phys. Rev. Lett. **81** (1998) 1782 [hep-ph/9805380].
- [2] M. Diehl, T. Gousset, B. Pire and O.V. Terayev, [hep-ph/9901233].
- [3] A. Freund, Phys. Rev. **D61** (2000) 074010 [hep-ph/9903489].
- [4] N. Kivel, L. Mankiewicz and M. V. Polyakov, Phys. Lett. **B467** (1999) 263 [hep-ph/9908334].
- [5] M.V. Polyakov, Nucl. Phys. Proc. Suppl. **79** (1999) 349 [hep-ph/9906261].
- [6] M.V. Polyakov and C. Weiss, Phys. Rev. **D60** (1999) 114017 [hep-ph/9902451].
- [7] M.V. Polyakov, Nucl. Phys. **B555** (1999) 231 [hep-ph/9809483].
- [8] M.V. Polyakov and C. Weiss, Phys. Rev. **D59** (1999) 091502 [hep-ph/9806390].
- [9] B. Lehmann-Dronke, P. V. Pobylitsa, M. V. Polyakov, A. Schäfer and K. Goetze, Phys. Lett. **B475** (2000) 147 [hep-ph/9910310].
- [10] B. Lehmann-Dronke, M. Maul, S. Schaefer, E. Stein and A. Schäfer, Phys. Lett. **B457** (1999) 207 [hep-ph/9901283].
- [11] M. Diehl, T. Gousset and B. Pire, [hep-ph/0003233].
- [12] D. Morgan and M.R. Pennington, Z. Phys. **C48** (1990) 623.
- [13] S.J. Brodsky and G.P. Lepage, Phys. Rev. **D24** (1981) 1808.
- [14] B. Andersson, G. Gustafson, G. Ingelman and T. Sjöstrand, Phys. Rept. **97** (1983) 31.
- [15] T. Sjöstrand, Comput. Phys. Commun. **82** (1994) 74.
- [16] B. Andersson and H. Hu, [hep-ph/9910285].
- [17] T. H. Bauer, R. D. Spital, D. R. Yennie and F. M. Pipkin, Rev. Mod. Phys. **50** (1978) 261; Erratum-ibid. **51** (1979) 407.
- [18] B. Badelek, M. Krawczyk, J. Kwiecinski and A. M. Stasto, [hep-ph/0001161].
- [19] G. Ingelman, A. Edin and J. Rathsman, Comput. Phys. Commun. **101** (1997) 108 [hep-ph/9605286].
- [20] E. Witten, Nucl. Phys. **B120** (1977) 189.
- [21] C. Peterson, T. F. Walsh and P. M. Zerwas, Nucl. Phys. **B174** (1980) 424.
- [22] P. Zerwas, Phys. Rev. **D10** (1974) 1485.
- [23] P. Aurenche *et al.*, [hep-ph/9601317].
- [24] M. Krawczyk, Acta Phys. Polon. **B28** (1997) 2659 [hep-ph/9712518].
- [25] M. Krawczyk, A. Zembrzuski and M. Staszal, [hep-ph/9806291].
- [26] C. F. von Weizsäcker, Z. Phys. **88** (1934) 612.
- [27] E. J. Williams, Phys. Rev. **45** (1934) 729.
- [28] C. Friberg and T. Sjöstrand, Eur. Phys. J. **C13** (2000) 151 [hep-ph/9907245].
- [29] G. A. Schuler and T. Sjöstrand, Z. Phys. **C68** (1995) 607 [hep-ph/9503384].
- [30] G. A. Schuler and T. Sjöstrand, Phys. Lett. **B376** (1996) 193 [hep-ph/9601282].
- [31] M. Diehl, T. Feldmann, P. Kroll and C. Vogt, Phys. Rev. **D61** (2000) 074029 [hep-ph/9912364].
- [32] B. Clerbaux and M. V. Polyakov, [hep-ph/0001332].
- [33] I. G. Knowles *et al.*, [hep-ph/9601212].
- [34] S. Chun and C. Buchanan, Phys. Rept. **292** (1998) 239.
- [35] B. Andersson, *The Lund Model*, Cambridge University Press 1998.
- [36] B. Andersson, G. Gustafson and B. Soderberg, Z. Phys. **C20** (1983) 317.
- [37] C. Caso *et al.*, Eur. Phys. J. **C3** (1998) 1.
- [38] A. Bramon, R. Escribano and M. D. Scadron, Eur. Phys. J. **C7** (1999) 271 [hep-ph/9711229].
- [39] T. Feldmann, P. Kroll and B. Stech, Phys. Rev. **D58** (1998) 114006 [hep-ph/9802409].
- [40] T. Feldmann, Int. J. Mod. Phys. **A15** (2000) 159 [hep-ph/9907491].
- [41] L. M. Barkov *et al.*, Nucl. Phys. **B256** (1985) 365.
- [42] D. Bisello *et al.* [DM2 Collaboration], Phys. Lett. **B220**, 321 (1989).
- [43] N. N. Achasov and A. A. Kozhevnikov, Phys. Rev. **D58** (1998) 097502 [hep-ph/9801308].
- [44] R. R. Akhmetshin *et al.* [CMD-2 Collaboration], [hep-ex/9904027].
- [45] G. J. Gounaris and J. J. Sakurai, Phys. Rev. Lett. **21** (1968) 244.
- [46] M. Aguilar-Benitez *et al.*, Phys. Lett. **B170** (1986) 1.
- [47] J. P. Perez-Y-Jorba and F. M. Renard, Phys. Rept. **31** (1977) 1.
- [48] S. Frixione, M.L. Mangano, P. Nason and G. Ridolfi, Phys. Lett. **B319** (1993) 339 [hep-ph/9310350].
- [49] S. Frixione and G. Ridolfi, Nucl. Phys. **B507** (1997) 315 [hep-ph/9707345].

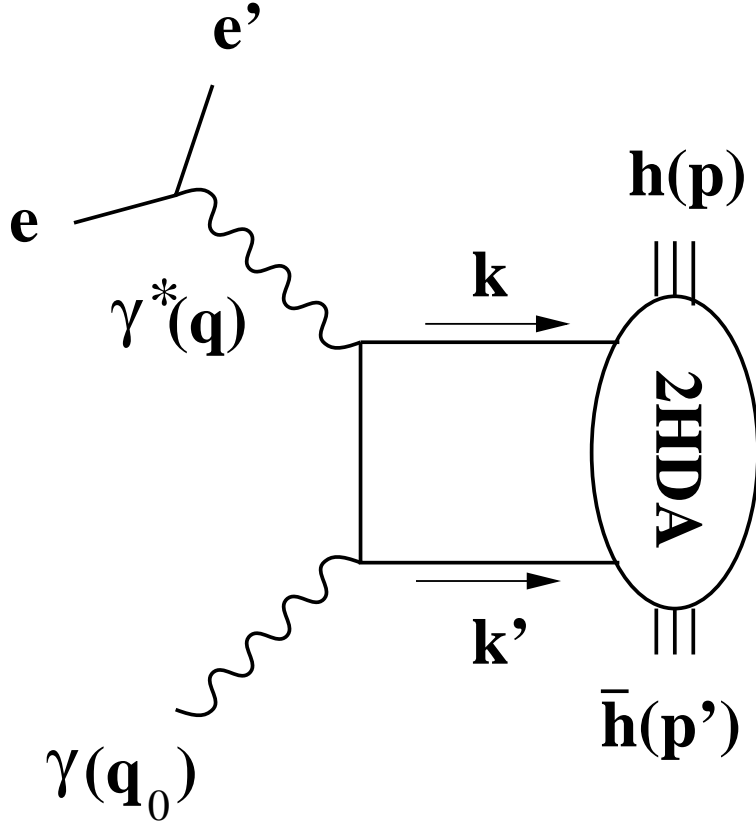


FIG. 1. Kinematics of the process $\gamma^* \gamma \rightarrow h \bar{h}$ and definition of the two-hadron distribution amplitude (2HDA).

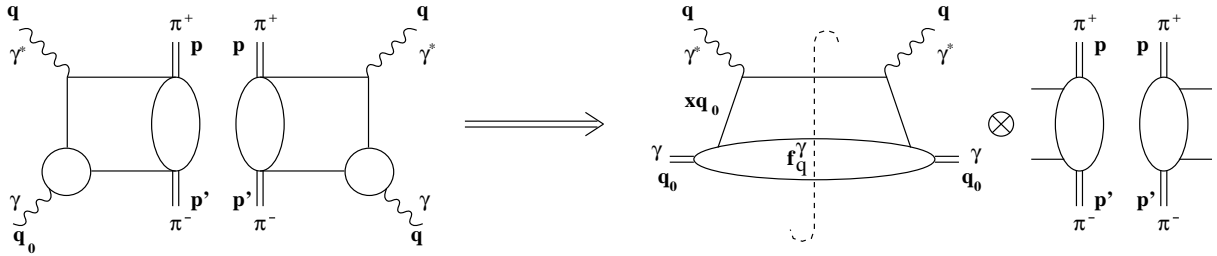


FIG. 2. Kinematical decomposition of the total cross section $\gamma^* \gamma \rightarrow \pi^+ \pi^-$ in terms of the hard scattering cross section $\gamma^* \gamma \rightarrow q \bar{q}$ and the transition probability $q \bar{q} \rightarrow \pi^+ \pi^-$.

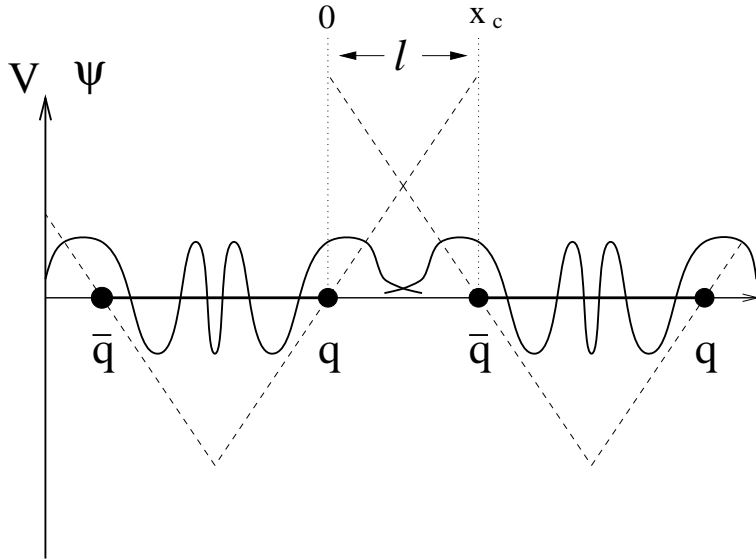


FIG. 3. Generation of transverse momentum p_{\perp} through the tunneling process. Displayed are the wave functions of the inner quark and the inner antiquark in the linear potential of the string. The region of exponential tunneling is of length $l = p_{\perp}/\kappa$, with κ being the string constant.

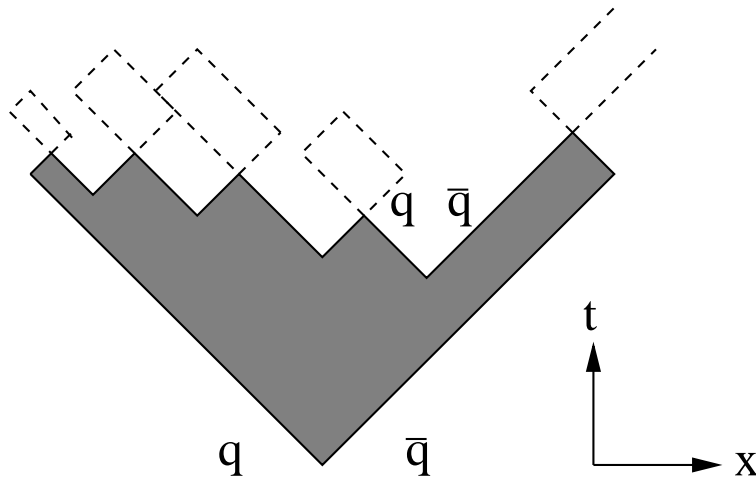


FIG. 4. Area law for the decay of a string into mesons in the Lund model: The decay probability of the string is proportional to $\exp(-b\mathcal{A})$, with \mathcal{A} being the shaded area in the x - t plane shown in the figure. The masses of the produced particles are proportional to the area surrounded by the dashed lines.

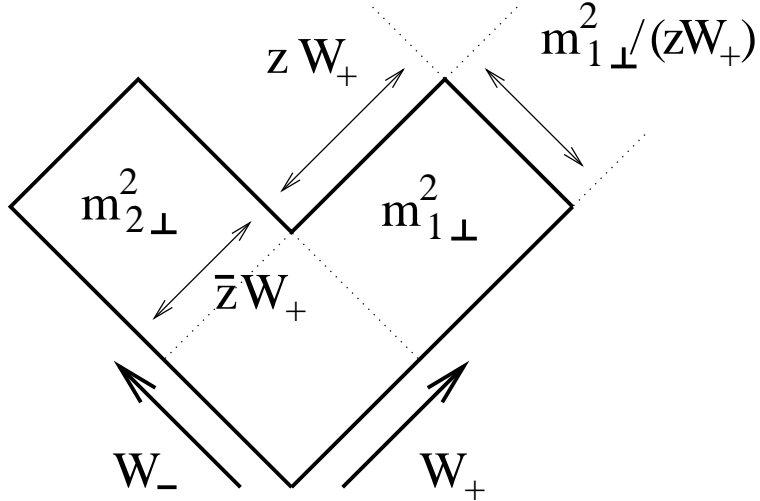


FIG. 5. The kinematical constraints for the string breaking into two pions. We have used the notation $\bar{z} = 1 - z$. W_+ and W_- are the momenta of the initial quark and antiquark in the $t-x$ plane. $W_+W_- = s$.

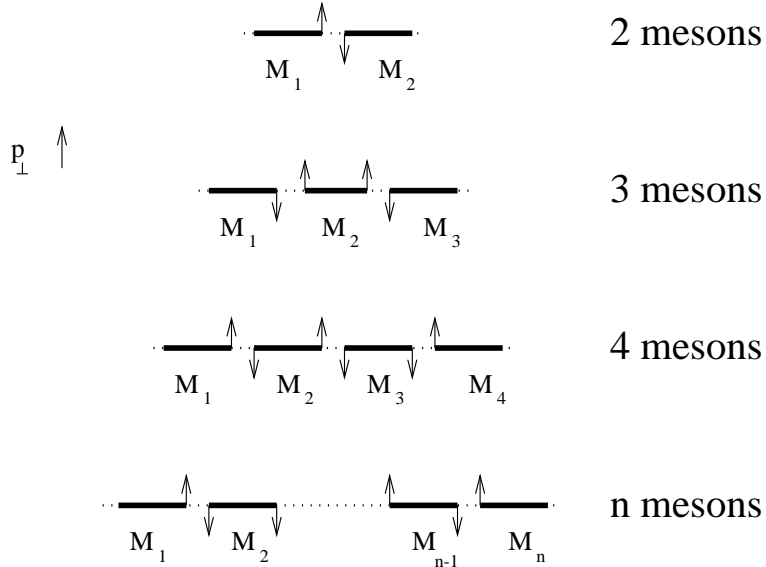


FIG. 6. Generation of the transverse momentum via string breaking. Particles at the two ends of the string receive only transverse momentum from one breakpoint, while those in the middle receive transverse momentum from two. So, the average transverse momentum for particles at the end is κ/π while it is $2\kappa/\pi$ for particles in a mid position.

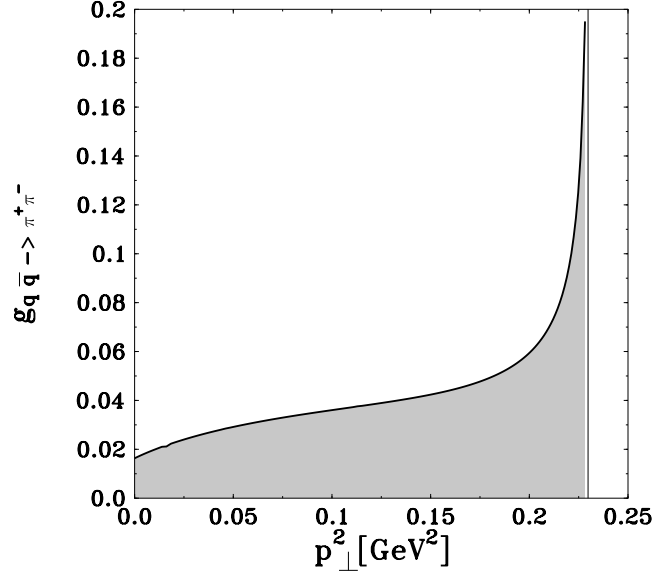


FIG. 7. The weight $g_{u\bar{u} \rightarrow \pi^+\pi^-}(s = 1 \text{ GeV}^2, p_{\perp}^2)$ as function of p_{\perp}^2 . The shaded area indicates the allowed region $s > 4m_{\pi_{\perp}}^2$ on the x -axis. The singularity at $s = 4m_{\pi_{\perp}}^2$ is integrable.

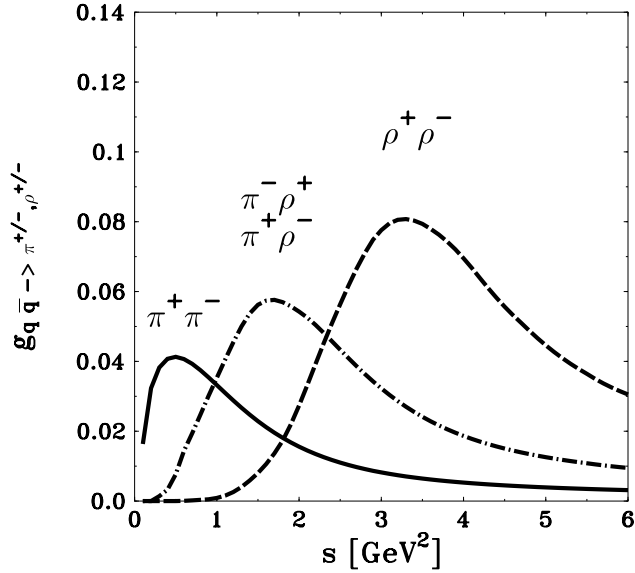


FIG. 8. The weights $g_{q\bar{q} \rightarrow \pi^{\pm}, \rho^{\pm}}$ as functions of s . The solid line shows the weights $g_{u\bar{u} \rightarrow \pi^+\pi^-}, g_{d\bar{d} \rightarrow \pi^+\pi^-}$, and the dashed line $g_{u\bar{u} \rightarrow \rho^+\rho^-}, g_{d\bar{d} \rightarrow \rho^+\rho^-}$. The dashed-dotted line represents the four weights $g_{u\bar{u} \rightarrow \pi^+\rho^-}, g_{u\bar{u} \rightarrow \rho^+\pi^-}, g_{d\bar{d} \rightarrow \pi^+\rho^-}, g_{d\bar{d} \rightarrow \rho^+\pi^-}$.

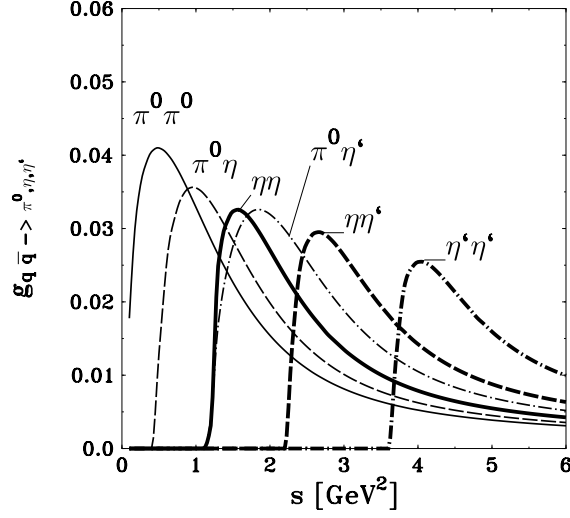


FIG. 9. The weights $g_{q\bar{q} \rightarrow \pi^0, \eta, \eta'}$ as functions of s , i.e. the contribution of neutral ($C = +$) pseudoscalar mesons. The following contributions are displayed:

- $g_{u\bar{u} \rightarrow \pi^0 \pi^0}, g_{d\bar{d} \rightarrow \pi^0 \pi^0}$ (thin solid);
- $g_{u\bar{u} \rightarrow \pi^0 \eta}, g_{d\bar{d} \rightarrow \pi^0 \eta}$ (thin dashed);
- $g_{u\bar{u} \rightarrow \pi^0 \eta'}, g_{d\bar{d} \rightarrow \pi^0 \eta'}$ (thin dashed-dotted);
- $g_{u\bar{u} \rightarrow \eta \eta}, g_{d\bar{d} \rightarrow \eta \eta}$ (bold solid);
- $g_{u\bar{u} \rightarrow \eta \eta'}, g_{d\bar{d} \rightarrow \eta \eta'}$ (bold dashed);
- $g_{u\bar{u} \rightarrow \eta' \eta'}, g_{d\bar{d} \rightarrow \eta' \eta'}$ (bold dashed-dotted).

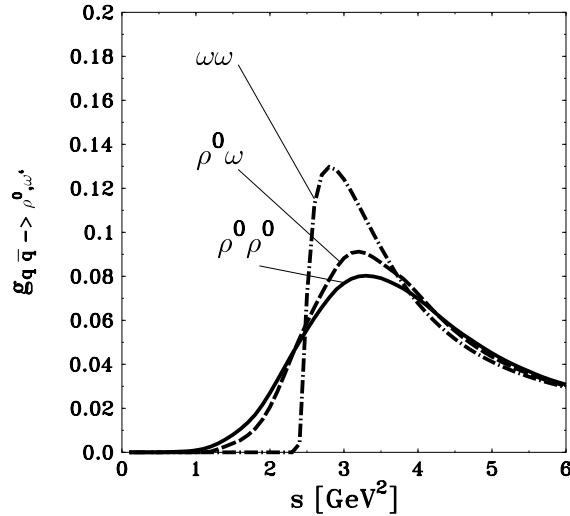


FIG. 10. The weights $g_{q\bar{q} \rightarrow \rho^0, \omega}$ as functions of s , i.e. the contribution of neutral ($C = -$) vector mesons. The following contributions as functions of s are displayed:

- $g_{u\bar{u} \rightarrow \rho^0 \rho^0}, g_{d\bar{d} \rightarrow \rho^0 \rho^0}$ (solid);
- $g_{u\bar{u} \rightarrow \rho^0 \omega}, g_{d\bar{d} \rightarrow \rho^0 \omega}$ (dashed);
- $g_{u\bar{u} \rightarrow \omega \omega}, g_{d\bar{d} \rightarrow \omega \omega}$ (dashed-dotted).

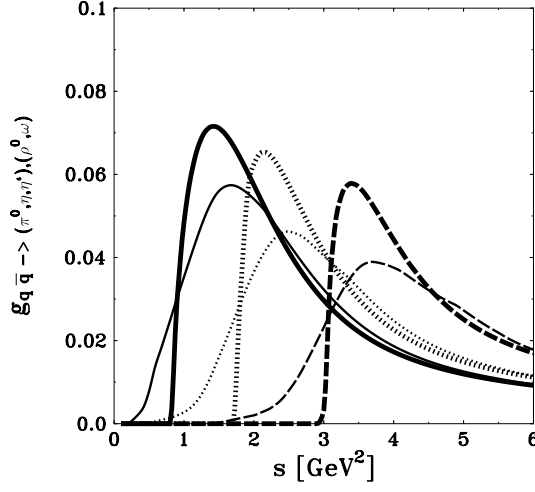


FIG. 11. The weights $g_{q\bar{q} \rightarrow (\pi^0, \eta, \eta'), (\rho^0, \omega)}$ as functions of s , i.e. the contribution of a pair of one pseudoscalar and one vector meson. The following contributions are displayed:

$g_{u\bar{u} \rightarrow \pi^0 \rho^0}, g_{d\bar{d} \rightarrow \pi^0 \rho^0}$ (thin solid);
 $g_{u\bar{u} \rightarrow \pi^0 \omega}, g_{d\bar{d} \rightarrow \pi^0 \omega}$ (bold solid);
 $g_{u\bar{u} \rightarrow \eta \rho^0}, g_{d\bar{d} \rightarrow \eta \rho^0}$ (thin dotted);
 $g_{u\bar{u} \rightarrow \eta \omega}, g_{d\bar{d} \rightarrow \eta \omega}$ (bold dotted);
 $g_{u\bar{u} \rightarrow \eta' \rho^0}, g_{d\bar{d} \rightarrow \eta' \rho^0}$ (thin dashed);
 $g_{u\bar{u} \rightarrow \eta' \omega}, g_{d\bar{d} \rightarrow \eta' \omega}$ (bold dashed).

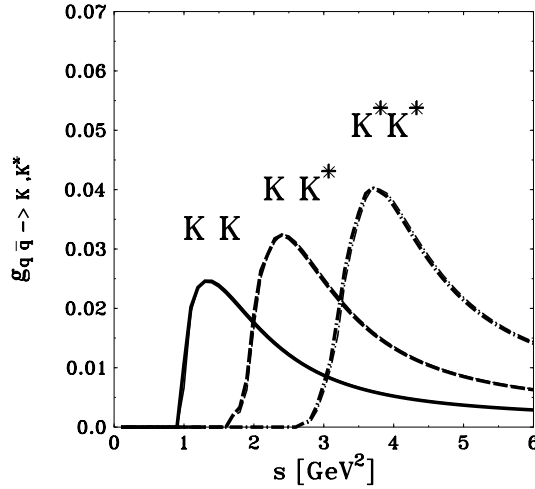


FIG. 12. The weights $g_{q\bar{q} \rightarrow K, K^*}$ as functions of s , i.e. the contribution of neutral and charged kaons. Because of being close together in their mass it is not possible to distinguish in the plot between charged and neutral kaons. The following contributions are displayed:

$g_{d\bar{d} \rightarrow K^0 K^0}, g_{u\bar{u} \rightarrow K^+ K^-}$ (solid);
 $g_{d\bar{d} \rightarrow K^0 K^{*0}}, g_{u\bar{u} \rightarrow K^+ K^{*-}}, g_{u\bar{u} \rightarrow K^- K^{*+}}$ (dashed);
 $g_{d\bar{d} \rightarrow K^{*0} K^{*0}}, g_{u\bar{u} \rightarrow K^{*+} K^{*-}}$ (dashed-dotted).

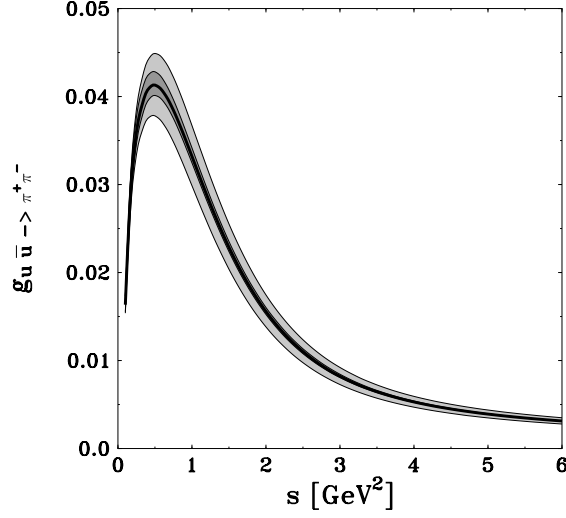


FIG. 13. Dependency of the function $g_{u\bar{u} \rightarrow \pi^+ \pi^-}(s)$ on the parameters a and b . The bold solid line shows the result for $a = 0.5$ and $b = 0.75 \text{ GeV}^{-2}$ as used in all calculations. The light grey area shows the variation from $a = 0.4$ to $a = 0.6$, while the dark grey area shows the variation from $b = 0.65 \text{ GeV}^{-2}$ to $b = 0.85 \text{ GeV}^{-2}$.

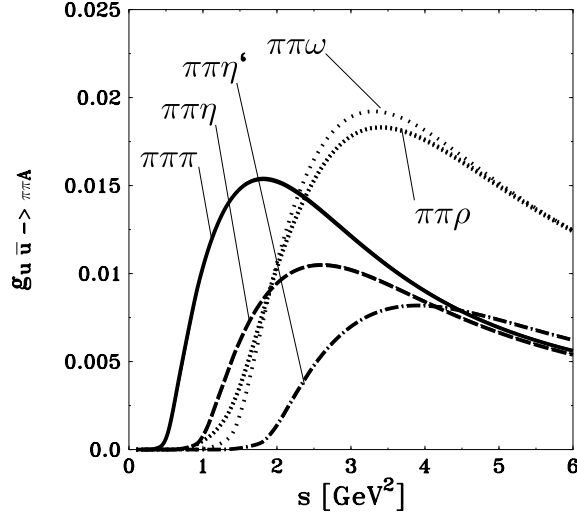


FIG. 14. The three-particle weights $g_{q\bar{q} \rightarrow \pi\pi A}$ as functions of s . The following contributions are displayed:
 $g_{u\bar{u}/d\bar{d} \rightarrow \pi^0 \pi^0 \pi^0}(s)$, $g_{u\bar{u}/d\bar{d} \rightarrow \pi^+ \pi^- \pi^0}(s)$ (solid);
 $g_{u\bar{u}/d\bar{d} \rightarrow \pi^0 \pi^0 \eta}(s)$, $g_{u\bar{u}/d\bar{d} \rightarrow \pi^+ \pi^- \eta}(s)$ (dashed);
 $g_{u\bar{u}/d\bar{d} \rightarrow \pi^0 \pi^0 \eta'}(s)$, $g_{u\bar{u}/d\bar{d} \rightarrow \pi^+ \pi^- \eta'}(s)$ (dashed-dotted);
 $g_{u\bar{u}/d\bar{d} \rightarrow \pi^+ \pi^- \rho^0}(s)$, $g_{u\bar{u}/d\bar{d} \rightarrow \pi^+ \pi^- \omega}(s)$, $g_{u\bar{u}/d\bar{d} \rightarrow \pi^- \pi^0 \rho^+}(s)$, $g_{u\bar{u}/d\bar{d} \rightarrow \pi^+ \pi^0 \rho^-}(s)$ (bold dotted).

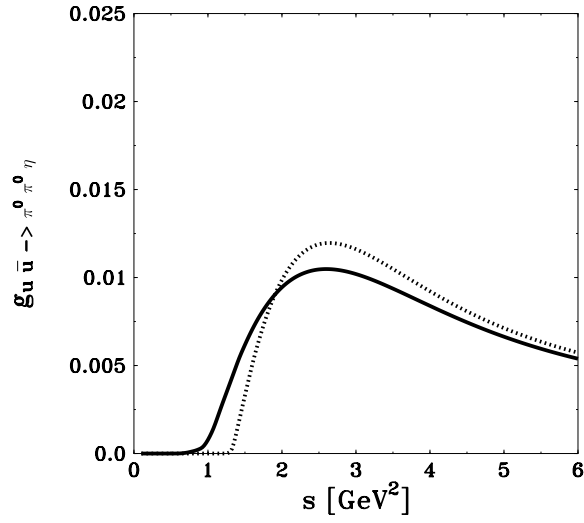


FIG. 15. Error of the approximation for the three-meson weights. The plot shows the weight $g_{u\bar{u} \rightarrow \pi^0 \pi^0 \eta}(s)$ calculated in two different ways. The solid line shows the form used in the calculations, where the heavier η meson is approximated. The dotted line shows the same result, but in a case where one of the two π^0 has been approximated.

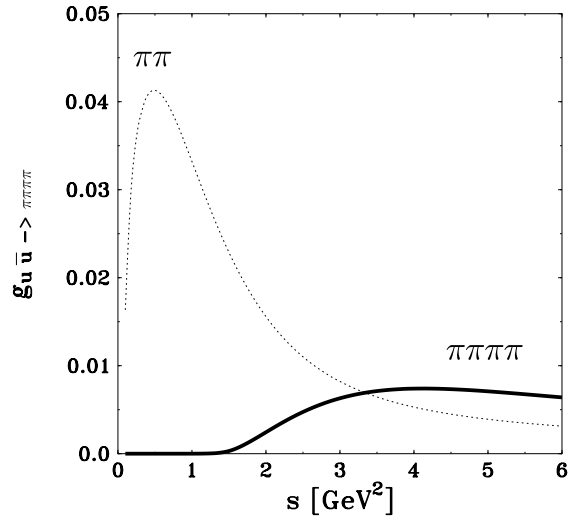


FIG. 16. Contribution of the four-meson weights as function of s . In the figure the weight $g_{u\bar{u} \rightarrow \pi^0 \pi^0 \pi^0 \pi^0}(s)$ is displayed (solid line) in comparison to the two-meson weight $g_{u\bar{u} \rightarrow \pi^+ \pi^-}$ (dotted line).

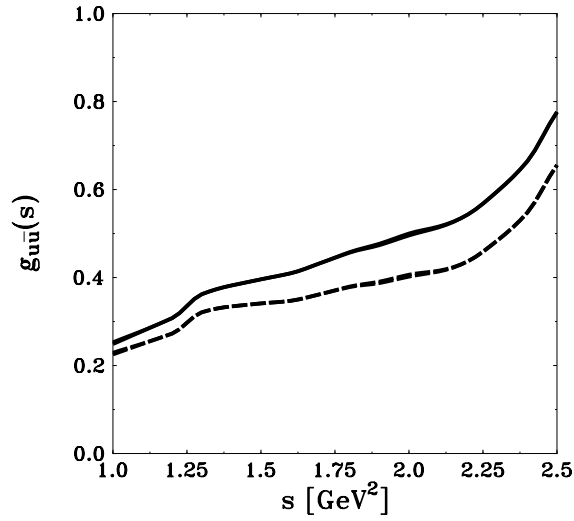


FIG. 17. The total weight in the small- s region. The solid line shows the function $g_{u\bar{u}/d\bar{d}}(s)$ as sum over all two- and three-meson weights. The sum over the two-meson weights $g_{u\bar{u}/d\bar{d}\rightarrow 2}$ alone is shown in the dashed line. One observes that the correction from the three-meson weights is substantial.

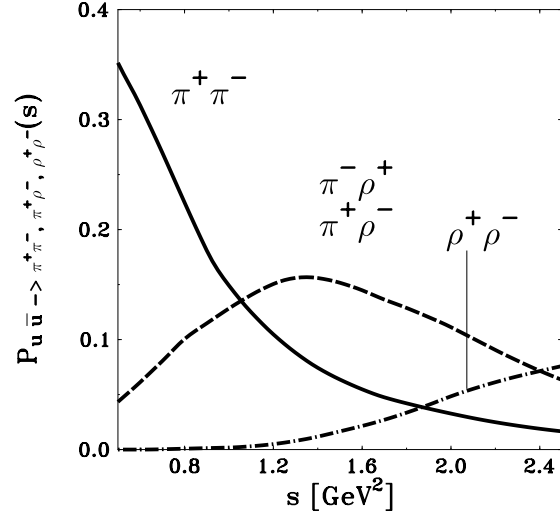


FIG. 18. The fragmentation probability $P_{u\bar{u}\rightarrow A}$ as function of s . The solid line shows the fragmentation probability for $A = \pi^+\pi^-$, the dashed line for $A = \rho^+\pi^-$ or $A = \rho^-\pi^+$, and the dashed-dotted line for $A = \rho^+\rho^-$.

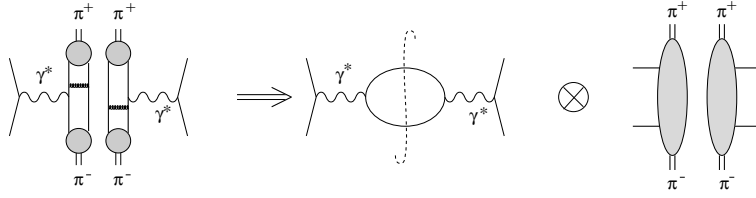


FIG. 19. Extraction of the fragmentation probability $P_{q\bar{q} \rightarrow \pi^+ \pi^-}(s)$ from the time-like pion form factor.

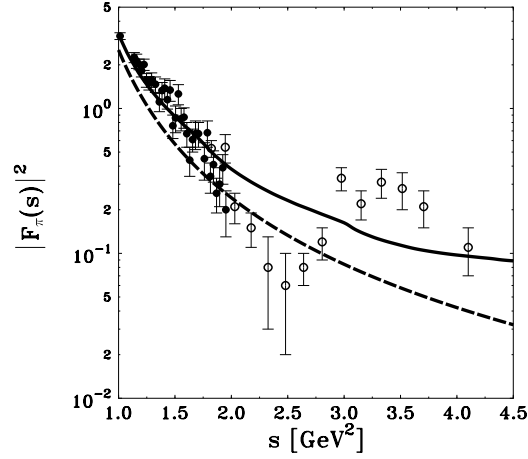


FIG. 20. Pion form factor $|F_\pi(s)|^2$ in the time-like region. The dashed line is the contribution from the decay of a single $\rho(770)$ resonance described in the VMD model. In the solid line we have added the contribution from string fragmentation into two pions. The filled circles are the NOVOSIBIRSK data and the open circles the data from the DM2 collaboration.

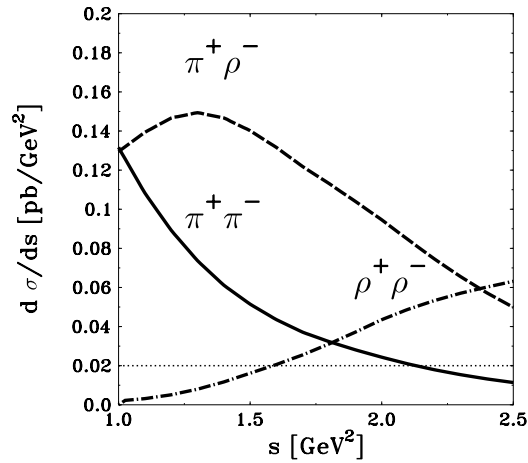


FIG. 21. Cross section $d\sigma/ds(e^+e^- \rightarrow e^+e^-A)$ as function of s with $A = \pi^+\pi^-$ (solid line), $A = \pi^+\rho^-$ (dashed line) and $A = \rho^+\rho^-$ (dashed-dotted line). The thin dotted line is the border for 10 events per unit in s for the LEP2 luminosity ($\mathcal{L} = 500 \text{ pb}^{-1}$). The c.m. energy for the two electrons is $\sqrt{S} = 175 \text{ GeV}$.

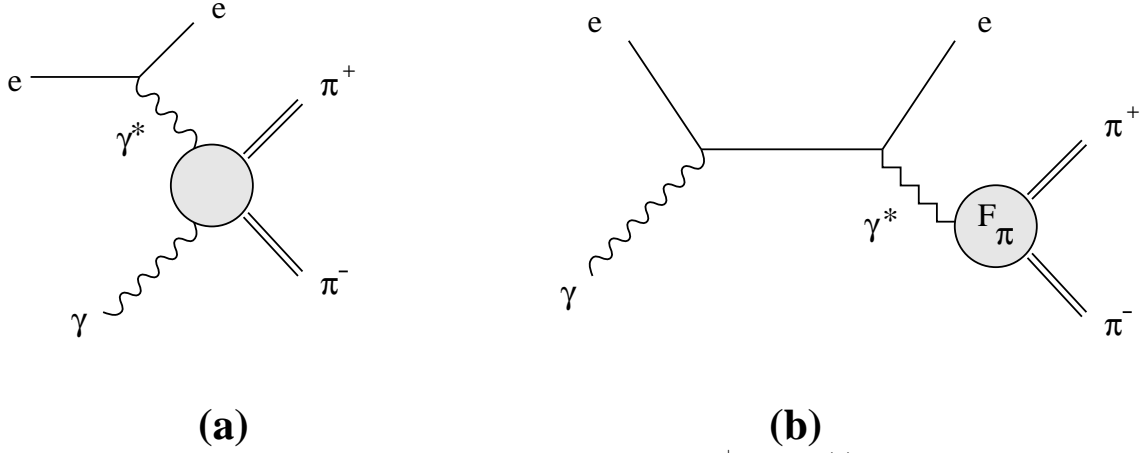


FIG. 22. Subprocesses contributing to the reaction $e + \gamma \rightarrow e + \pi^+ + \pi^-$: (a) pion pair production via $\gamma^*\gamma$ scattering, (b) via bremsstrahlung.

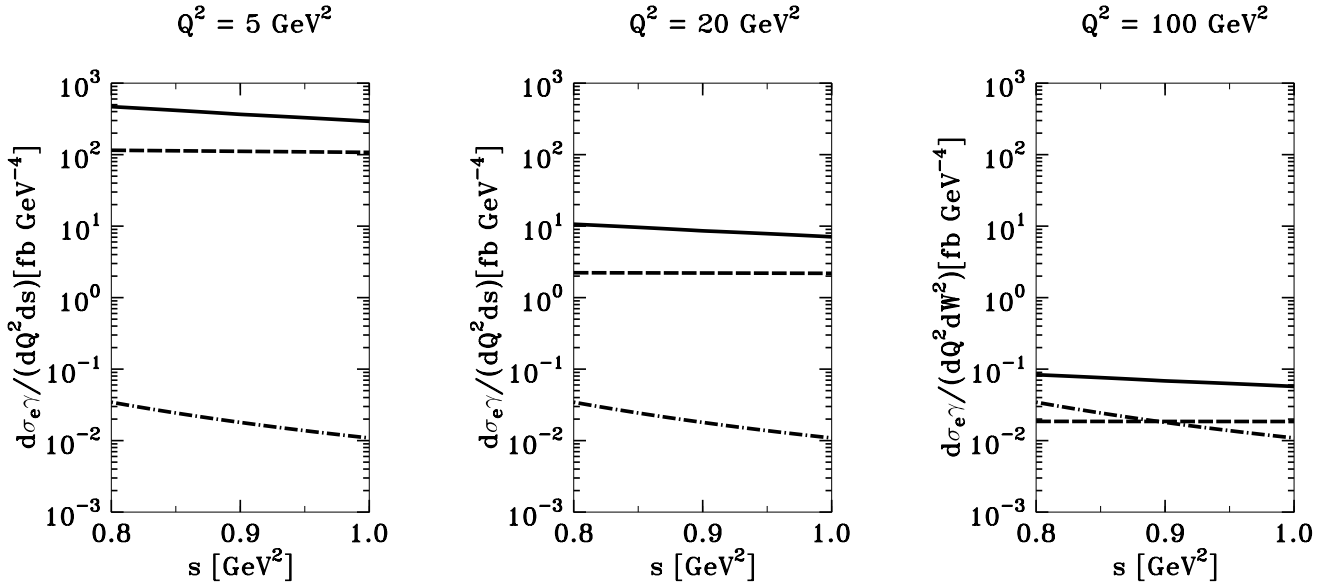


FIG. 23. Comparison of the Lund model calculation (solid line) with the model given in Ref. [11] (dashed line) for the cross section $d\sigma_{e\gamma}/(dQ^2 ds)$ for three different values of Q^2 as function of s . The dashed dotted line shows the contribution of the bremsstrahlung process as given in Ref. [11]. For the invariant mass of the electron photon system we have taken in all figures the value $\sqrt{S_{e\gamma}} = 60$ GeV.

	strangeness $S = 0$ mesons	strangeness $S = 1$ mesons
charged	$\pi^+\pi^-; \rho^+\rho^-$ $\pi^+\rho^-; \rho^+\pi^-$	$K^+K^-; K^{*+}K^{*-}$ $K^{*+}K^-; K^+K^{*-}$
neutral	all $C = +- $ meson combinations: π^0, η, η' all $C = -- $ meson combinations: ρ^0, ω	$K^0\bar{K}^0; K^{*0}\bar{K}^{*0}$ $K^{*0}\bar{K}^0; K^0\bar{K}^{*0}$

TABLE I. The possible combinations for exclusive two-meson production in $\gamma^*\gamma$ scattering, if the primary quark-antiquark pair is $d\bar{d}$ or $u\bar{u}$.

particle	mass m [GeV]	width Γ [GeV]
π^\pm	0.13957	–
π^0	0.13498	–
ρ^\pm	0.76690	0.14900
ρ^0	0.76850	0.15100
K^\pm	0.49360	–
K^0	0.49767	–
$K^{*\pm}$	0.89160	0.04980
K^{*0}	0.89160	0.05050
η	0.54745	–
η'	0.95777	–
ω	0.78194	0.00843

TABLE II. Masses and widths used for calculating $g_{u\bar{u}}(s)$. In case no number is given for the width, it has been neglected in the calculation.